# Evaluation of Microstructure and Hot Corrosion Behaviour of YPSZ / $Al_2O_3$Composite Plasma Sprayed Coatings at 900°c by Molteneutectic vanadate-SulfateSalt

**Mohammed J Kadhim, Sami A Ajeel, and Ali M Resen**

Department of Production Engineering and Metallurgy, University of Technology, Baghdad, Iraq

## Abstract

This work is aimed to study effect of alumina coating on the partially stabilized zirconia alumina composite (YPSZ/ $Al_2O_3$) on the microstructure, phase transformation and hot corrosion performance of eutectic molten salt $V_2O_5$ + 45 wt% $Na_2SO_4$ and comparing with conventional YSZ.Both the pure alumina and YPSZ are sprayed by using atmospheric plasma spray APS. Hot corrosion for composite is done by exposing the samples to an isothermal air furnace testing at900 °C for different exposure times of40 and 80 hours. Upper surface plan views of the coatings are examined using SEM. The hot corrosion test products are determined using EDS, EPMA and XRD. The results indicate the higher hot corrosion resistance of YSZ/ $Al_2O_3$composite coatings compared with conventional YSZ sprayed coatings. Degradation of YSZ due to the presence of eutectic harsh salt attack is occurred by destabilization of yttria from the zirconia yttria coatings. This will lead to disrupt transformation from metastable tetragonal phase (t') to monoclinic phase (m). the corrosion products of $YVO_4$produce by leaching process. During exposure the composite to the molten salt the $Al_2O_3$is reacted with vanadate to form a low-melting liquid eutectic phase, leading to dissolution of $Al_2O_3$in molten $NaVO_3Na_2O–V_2O_5–Al_2O_3$. The pores and cracks within the YSZ coating are filled with $Al_2O_3$. The absences of leaching of yttria in under layer for composite coatings is related to the absence of pockets of open porosity and cracks due to elimination after alumina layer applied.

**Keywords:** yttria partially stabilized zirconia; Plasma sprayed coatings; hot corrosion; vanadate-sulfate.

## 1. Introduction

Thermal barrier coatings (TBCs) consist a zirconia based ceramic top coat over an intermediate MCrAlY(M5Ni, Co, Fe) bond coating, are extensively used in gas turbines in hot sections such as blades and vanes of gas turbine engines and isolation unit of fuel in oil refineries. These coatings increase the operating temperature and enhance the durability of components and the engine efficiency subsequently [1-4].The top coat acts as a thermal insulation layer, while the bond coat provides corrosion and oxidation protection for the substrate and improves the adhesion of the ceramic top coat to the metallic substrate[3-7].

Hot corrosion is common failure mode of TBCs which used in land-based industrial engines and sea engines which are usually operated with low-quality fuels containing sulfur and vanadium [8,9]. During service, molten salts such as Na, S and V, and corrosive gases attack the TBC system. yttria is leached out of zirconia to form YVO4 by reaction with NaVO3or V2O5. These reaction leads to the structural transformation of zirconia from the tetragonal to the monoclinic phase. The structural destabilization of ZrO2 is accompanied by a large destructive volume change, leading to large stresses within YSZ, which eventually results in delamination and spalling of coatings [10-14].Many researchers[15-18] study the method to reduce hot corrosion and enhancement the performance of TBCs in harsh environments by stabilized zirconia with oxides such as india(In2O3), scandia (Sc2O3), tantalic oxide (Ta2O5), and ceria (CeO2).

The aim of this study investigate the effects of alumina addition on hot corrosion of TBCs, both the monolithic YSZ coating and the composite YSZ/Al2O3 system will be exposed to the molten saltV2O5 + 45 wt%Na2SO4at 900oC. The microstructure, phase analyses and hot corrosion mechanism of composite will be studied.

## 2. Materials and methods

### 2.1 Materials

A stainless Steel 316Lplate with dimensions of 15* 24* 3.2 is used as the substrate material. The Ni-22Cr-10Al-1.0Y (wt.%) type metallic powder (AMDRY 962) is used as the bond coat layer with particles size of 53–106μm. The ceramics powders used for the top coat areZrO2-7 wt.% Y2O3(Amperit 827.007) with spherical particles ranging in size from 16 to 90 μm and Sulzer Metco

105SFP(99.5wt% Al2O3) with Nominal range of -31 +3.9 µm.

### 2.2 Air plasma spraying

Thermal barrier coatings (TBCs)are fabricated by a Metco 6MR air plasma spray system using Sulzer-Metco 3-MB plasma gun(Sulzer Metco AG, Switzerland). The feedstock powders are fed with Twin-system 3-ME. Prior to the coating deposition, the substrate surface is grit-blasted in a sand-blasting box using the alumina abrasive of 24 meshes, under a pressure of 5 bars and a distance of 15 cm. During spraying, the substrate and coatings are cooled using the compressed air. The metallic bond coating deposited with a thickness of approximately 150 µm. The ceramic coatings thicknesses are 350µm and 150 µm for YPSZ and Al2O3 respectively. Details of the spraying parameters are summarized in Table 1.

**Table 1 plasma spraying parameters**

| Spray parameter | Bond layer | Ceramic layer |
|---|---|---|
| Primary gas | Ar | Ar |
| Pressure,psi | 100 | 100 |
| Flow,SCFH* | 80 | 70 |
| Secondary gas | $H_2$ | $H_2$ |
| Pressure,psi | 50 | 50 |
| Flow,SCFH | 15 | 15 |
| Current,A | 450 | 500 |
| Voltage,volt | 50 | 55 |
| Spray distance,cm | 12 | 8 |
| Angle,% | 90° | 90° |
| Carrier | Ar | Ar |
| Flow,SCFH* | 28 | 37 |
| Spray rate , 1b/h | 10 | 10 |

SCFH* Standard feet Per Hour

### 2.3 Hot corrosion testing

Hot corrosion resistance of both the as sprayed YSZ coating and the composite YSZ/ Al2O3areheatedto 900 oC for different times of 40 and 80 hours. Coatings are exposed to the mixture of 45 wt% Na2SO4+ 55 wt% V2O5 in order to simulate the deposits and the temperature present in a diesel engine combustion chamber. The corrosive powder is placed on the surface of coatings in a 25

mg/cm2concentration. Where powder is diluted in delisted water with ratio is 20%.

### 2.4 Specimens characterization

The features, Morphology and microstructure of both the monolithic YSZ coating and the composite YSZ/Al2O3 system after and before hot corrosion test are determined by Visual examination and optical microscopy (type: Olympic; Model Versamet3, Union Co, Japan) and Scanning Electron Microscope (type: VEGA\TESCAN (Czech Republic)).

X-ray diffraction is used in phase identification phase analysis. The coating phase structures are characterised by X-ray diffractometer (XRD type, D8 ADVANCE, Bruker, Germany) using CuKα radiation (λ = 1.5406 Ao) with the step scan is 0.2oand step time of 1.2 s. the energy dispersive spectroscopy (EDS) is used as a complement of XRD for local element analysis and detection of corrosion products. The surface roughness (Ra) of YSZ coating is measured by a Mitutoyo Surftestprofilometer (Mitutoyo SJ-201P, Japan) with a cut-off length of 800 μm and a measurement length of 4 mm. The roughness reported is the average of five values scanned from different areas on the coating surface.

## 3. Results and discussion

### 3.1. Characterization of coatings before and after hot corrosion test

Figure 1 shows the visual image of both types of coatings as a sprayed. It indicates that the colour of YSZ is light yellow, while for YSZ/Al2O3 is light gray.After the hot corrosion test, the coating colours change from yellow color to dark-brown for YSZ and from light grey to become brown for YSZ/Al2O3. The failure of sprayed coating as observed from the naked eye demonstrates that the detachment occurred in the top ceramic coat/ bond coat interface (YSZ/ bond interface). Sign of separation is started at YSZ sprayed coating after 80 h exposure at 900oC. It appears that the failure at the interface between YSZ/bond coats is due to buildup of TGO where the cracking initiated at this region; this is confirmed by many researchers[19-21]. A slightly damaged presenting increases with increased exposure time to make large portions of spalled material in alumina coating. In addition to that, alumina coating

3observed more resistance to hot corrosion and no spalled from the substrate with some of crack are observed at surface. Also observed by

naked eye, no detachment and color changing which supported the lower reaction time (1 Hour) of the corrosive compounds with sealed coatings.

Figure 2 presents the surface morphology of both the monolithic YSZ coating and the composite YSZ/Al2O3 system. This figure indicates the presence of the two kinds of microstructure in both coating systems. One referred to the partially melted particles, which had a porous microstructure, and the molten parts bonded with each other to form a dense structure.

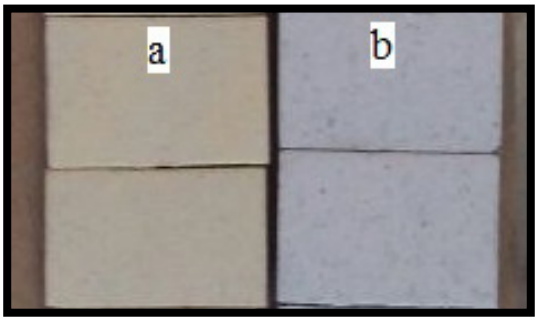


**Figure 1:Visual image of the top surface of the plasma-sprayed the monolithic YSZ a), b) YSZ/Al2O3 composite.**

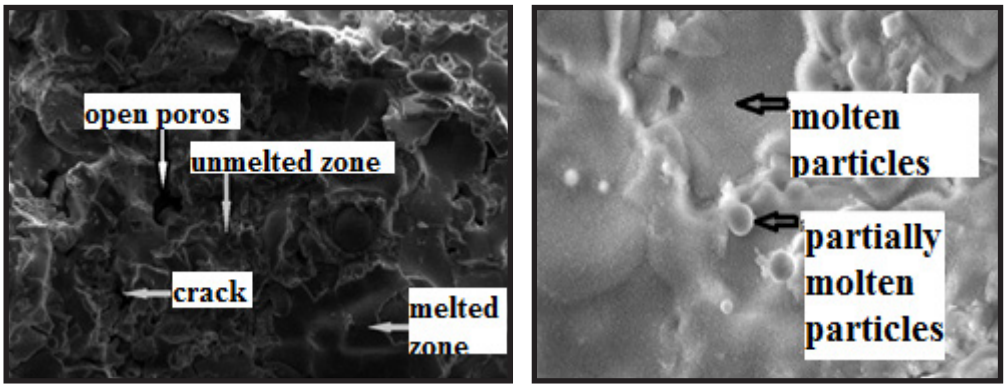


**Figure 2: SEM micrographs of the top surface of the plasma-sprayed the monolithic YSZ a), b)YSZ/Al2O3 composite.**

The surface roughness (Ra) of the monolithic YSZ and YSZ/Al2O3composite coatings are 6.28µm and 3.26µm respectively. This result indicates that the alumina coating has smother surface than monolithic YSZ. This difference is due to the amount of existence of micro cracks and partially molten particles in YSZ more than in YSZ/Al2O3composite involved in the lover deformation impact of the surface as compared with the fully molten particles for YSZ/Al2O3.

### 3.2 Phase analysis of coatings before hot corrosion

Fig.3 illustrates the XRD patterns of coatings before the corrosion test. It demonstrates that the phase composition of YSZ coatings is the non-transformable tetragonal phase (T/) with small amount of (m) phase

This phenomenon is resulted from the rapid solidification during the process plasma spray [22,23]. X-ray diffraction peak of plasma sprayed coating of YSZ/Al2O3 overlay ceramic top coating is consisted of rhombohedral (α) phase of Al2O3 with some of orthorhombic (γ) phase.

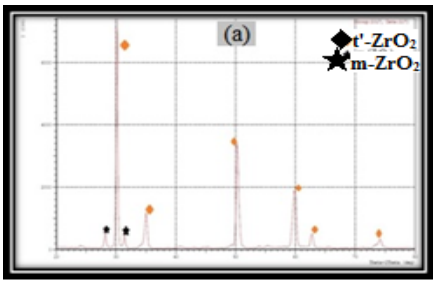


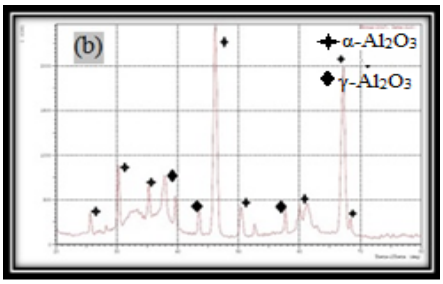


### 3.3. Hot corrosion behavior

#### 3.3.1. Microscopic surface examination

Figures (4 and 5) show the SEM image of plan view of coatings after hot corrosion at different times for both coatings. SEM micrographs indicateporous surface with the severe formation of agglomerated crystals with different shapes. These structures include rod-like and semi cubic crystals as clearly shown in figures 4 and 5. Where rod-type or like needle crystals (B) and the semi-cubic (C) have been formed on the porous coating surface (A). It is observed that the size of both crystals growth with time exposure. The size of these crystals is decrease with alumina coating [24,25]. Comparing between these figures, it can be observed that a considerable change in morphology of the surface for Al2O3 overlay after 40h. Coarse acicular shaped α-Al2O3crystals are present at low exposure time transform to faceted crystals, and the directionality of the crystals is varied from region to other. It also, observes dissolution of grain boundaries. These features are agreement with other researches [25-28]. Low exposure time indicates fewer of corrosion product crystal that is due to low time to permit for reaction to occurs. With increasing of reaction time, both structure of matrix and harmful

product are changed, where the surface will increase roughness and the boundary between grains is represented as pores. These structures are due to reaction of molten salt with yattria leaving the porosity [29-31]. The percent of porosity is increased at 80h. Finally the corrosion product becomes more size after it is small and numerous figure 4 and 5

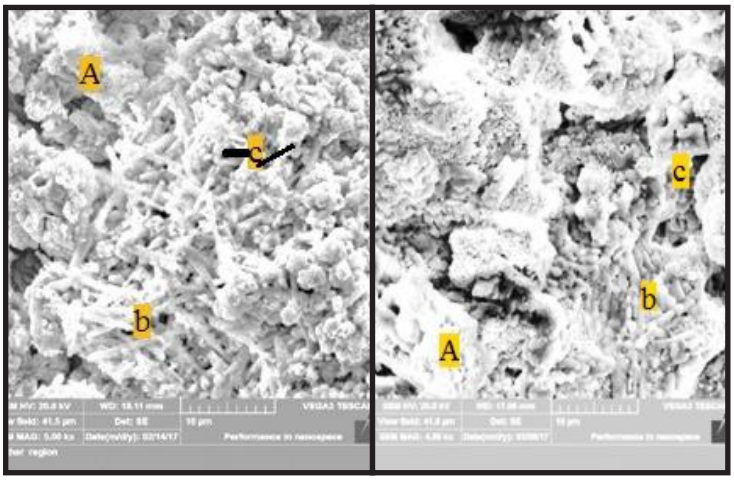


**Figure 4 :SEM micrographs of top surface of coatings for 100%YSZ after (a) 40 h, and (b) 80 h.**

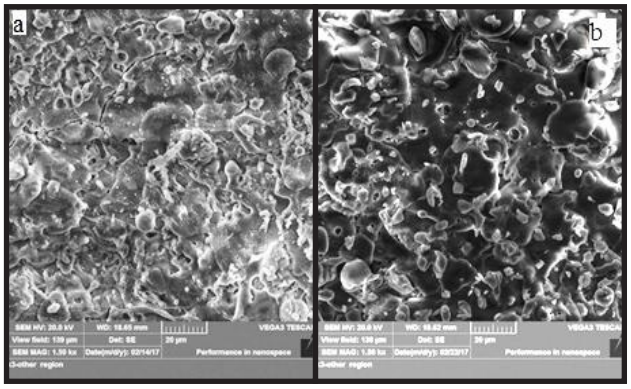


**Figure 5: SEM micrographs of top surface alumina coatings after (a)40 h, and (b) 80 h.**

The EDS analysis is performed at different regions of the coating surfaces to confirm the chemical compositions of the hot corrosions products. The EDS analysis demonstrates for that the crystals are composed of yttrium, vanadium, aluminium and oxygen as shown in figures 6, 7 and 8. XRD analysis patterns of coatings confirmed the

presence of these phases are YVO4 (Fig. 9). For the YSZ TBC coating, after hot corrosion tests for 80 h, degradation and spallation occurs, Fig.9ashows Porous structure formed on the YSZ coating as result to the damage caused by Na2SO4 + V2O5 [32]. Also the phase analysis XRD patterns for YSZ coating indicate large amount of tetragonal zirconia phase on the surfaces of YSZ coating transformed to monoclinic phase. This transformation results from depletion of yttria [33]. In addition, significant quantity of rod/plate shaped as a product of hot corrosion reaction, YVO4, is indicated on the surface of the YSZ coating (fig 6). These results agree with results reported by other researchers[10,19,31]. The amounts of these phases increase with increasing interaction time. Increasing these phases are resulted in reducing the t' phase with producing m phase. For YSZ/Al2O-3composite coatings EDS analysis are obtained to contain Al , O , Y and Zr; Y, V and O are semi-cubic and rod crystals of mixture of YVO4 as shown in figs.(7 and 8). The Zr and O or Al and or even Y, Zr, Al and O compose of base composition and formation from hot corrosion such as acicular-shaped crystals of alumina which result from hot corrosion. The amounts of these phases are also related directly to exposure time and type of composition as shown in figures (7 and 8).

The presence of alumina results in reducing quantity of corrosion product and the size of it. This change is attributed to increasing of corrosion resistance, the structure base coating changes from small grain of YSZ for to dendritic structure with some of acicular-shaped crystals as shown in fig10.

The first stage of corrosion producing the corrosive salt V2O5-Na2SO4presents the formation of these two compounds and then finally the formation of the eutectic mixture (55 wt% V2O5 and 45 wt. % Na2SO4 which condensed on the plasma sprayed thermal barrier coatings [32,33]. The fuel is contaminated with sulfur (S) and vanadium (V). The compounds of these elements are formed due to the reaction of S with Na (NaSO4) and oxygen with V (V2O5) respectively [32].As shown in the following equation:

$$V_2O_5 + Na_2SO_4 \rightarrow 2(NaVO_3) + SO_3 \quad \ldots\ldots\ldots (1)$$

This compound is reacted with yttria (the stabilizer for zirconia) and led to the formation of low melting yttrium vanadates (V2O5YV04) [34].which is

highly corrosive. The NaVO3 is reacted with Y2O3. This reaction causes destabilization of zirconia by converting from tetragonal to monoclinic phase. as a result, cracking and spallation of YSZ as the follow [31, 34].

ZrO2(Y2O3)(t + 2(NaVO3) → ZrO2 (monoclinic) + 2YVO4+Na2O …..(2)

Results also show no indications to form compounds based contained vanadium, sulfur, sodium or chlorine is formed. No evidence from EDS and X-ray diffraction analyses are found to confirm the chemical reaction between Na2SO4 and YSZ or YSZAl had progressed; these results are agreement with results of other researches [30, 32]. The other observation is that the absence of any compounds contained sodium is formed. This is clearly revealed that the fierce compound is V2O5 rather than Na2SO4. It is still Na2SO4 played a role to form the harmful phases [8,9,30]. Although, the formation of harmful compounds of YVO4 may involve the presence of Na2SO4, the absence of detection any sodium element in EDS analysis may due to the sublimit at high temperature of Na2O [38].

Also Na3VO3 can react with alumina to form sodium vanadium aluminates AlVO4. the reason for degradation of Al2O3 during exposure to hot molten sulfate–vanadate salt is the liquid phases consisted of Al, Na, V, and O formed at temperature exceeds 610oC. Therefore, it is deduced formation of low-melting liquid phase. This phase is accountable on failure of the Al2O3 overlay at hot corrosion testing. This notion can be confirmed by the further evidence in the present study. The surface of Al2O3 overlay coating have ‘‘cauliflower’’ morphology before hot corrosion is begun (Fig. 10), whereas after hot corrosion testing have acicular-shaped and faceted crystals. In addition, we can observe gap between the crystals. When pure Al2O3 co-existed with NaVO3 at 900 oC, the low melting liquid phase is formed. This phase is contained Al, Na, V, and O. The continuous formation of that phase can result losing of integrity of the coating surface. Through cooling process, the liquid phase decomposes and Al2O3 crystal form crystals on the surface of the Al2O3 overlay (Fig. 10)[30]. Further of corrosion is etched the subsurface region and caused the grooves. However, AlVO4 corrosion product is not found at the composite Al2O3 /YSZ coating when exposure to molten sulfate–vanadate salt for 80h.

**That is due to decompose of AlVO4 to form Al2O3 crystals on the surface of the overlay.**

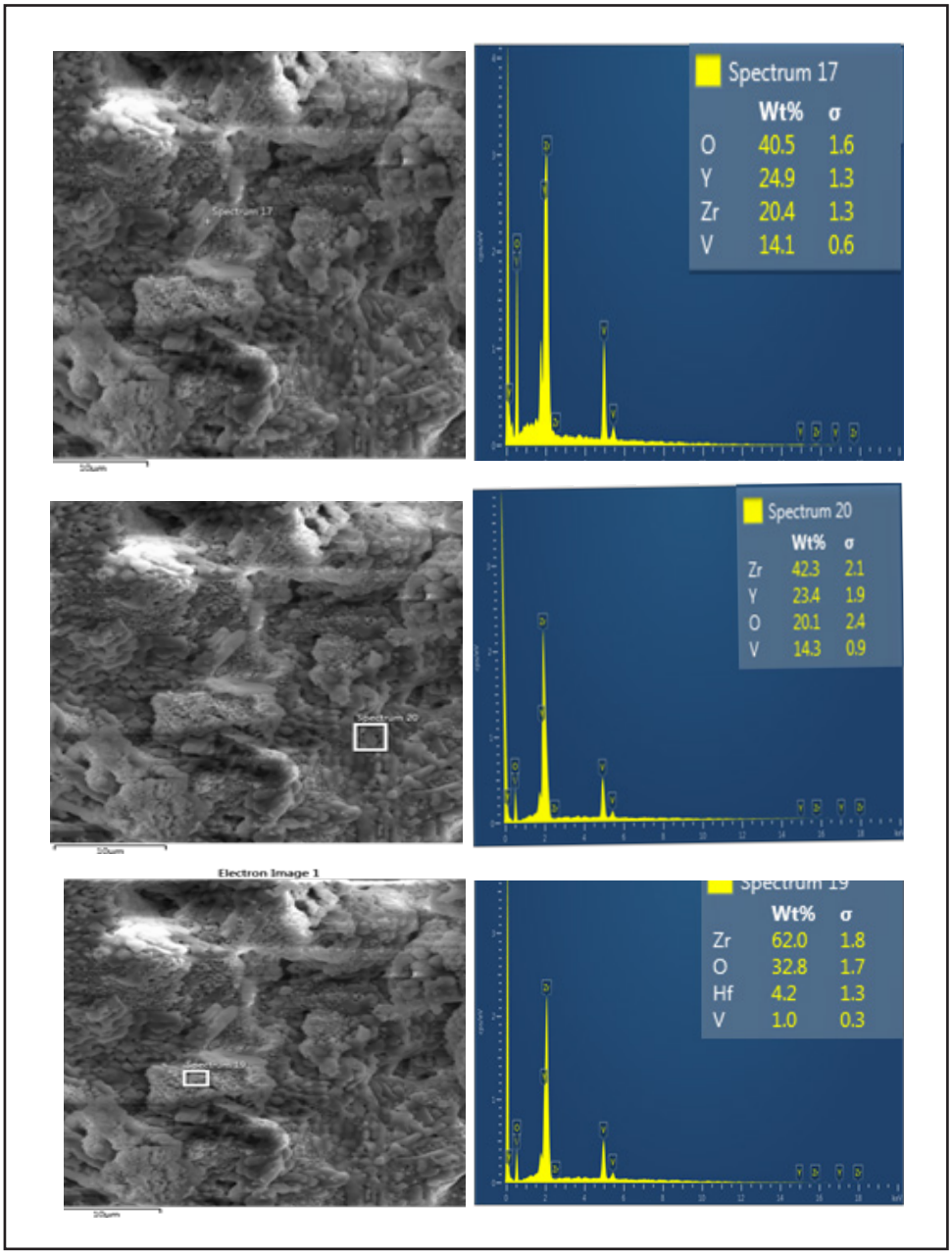


**Fig. 6 :The EDS analysis for different shape crystals for YSZ at 80h.**

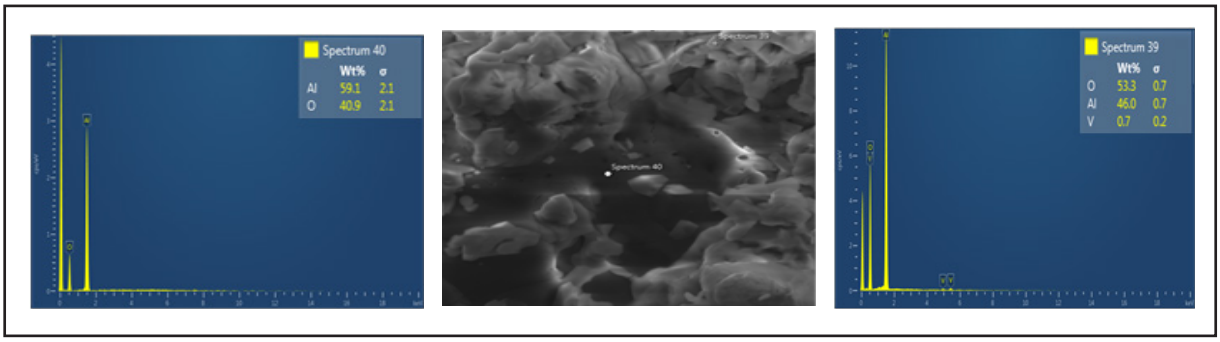


**Fig. 7: The EDS analysis demonstrated for different shape crystals for YSZ/Al2O3composite coatings at 40h.**

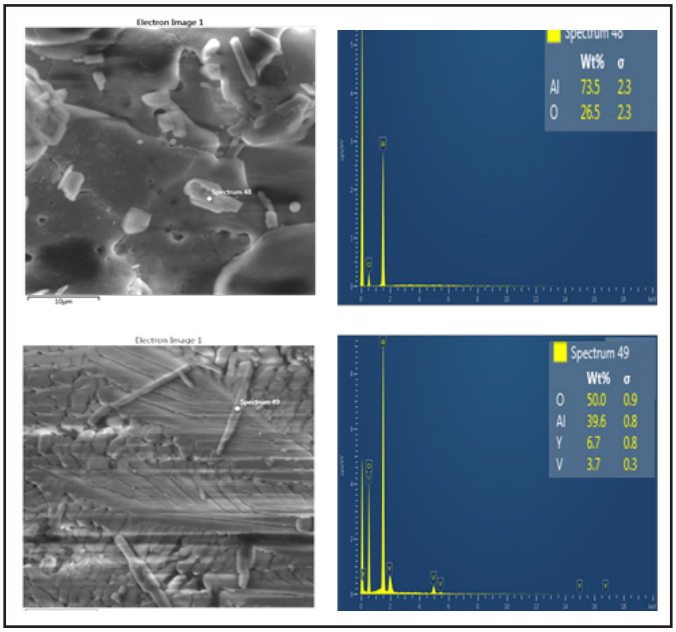


**Fig.8 : The EDS of YSZ/Al2O3composite coatings at 80h.**

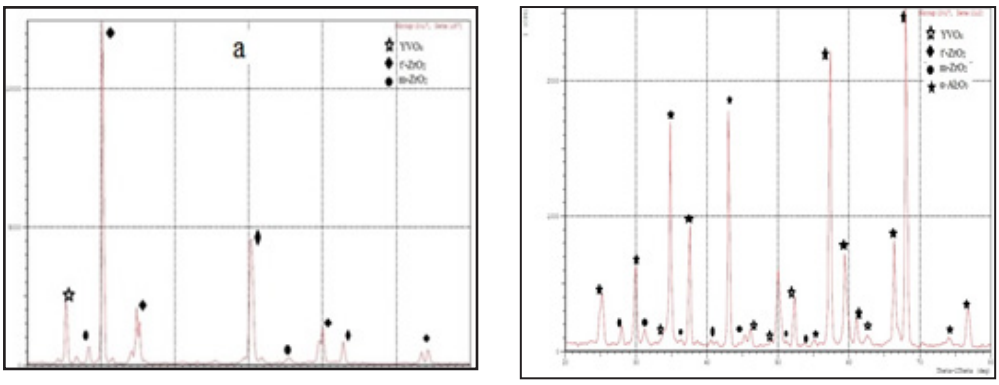


**Fig. 9 :XRD analysis patterns of coatings (a) YSZ,(b) YSZ/Al2O-3composite coatingsat 80hr.**

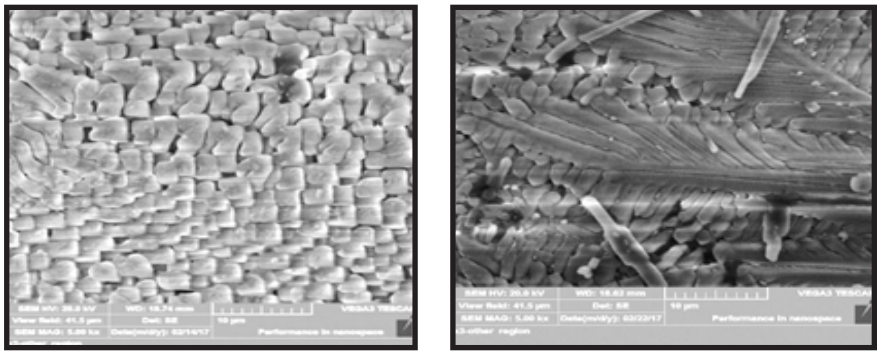

**Figure 10: The structure of YSZ/Al2O3composite coatingsat interaction time 10h (a) and 80 h(b).**

**4. conclusions**

1- Using of air plasma spray (APS) technique is successfully process to produce the thermal barrier coatings. This process is done by carefully selecting of processing sheet to produce perfect thermal plasma spray coatings

2- Using the alumina coating is resulted in high reduction of open porosity percentage at the upper surface which led to decrease surface roughness and filtration of the molten salt to bond layer.

3- The X-ray diffraction of plasma sprayed coatings showing the dominate phases of YSZ is t'-phase with small amount of m-phase, while for YSZ/Al2O3composite coating the phases are rhombohedral (α) phase of Al2O3 with some of remaining orthorhombic (γ) phase.

4- The high stability of alumina is more than t'-phase at the same temperature.

5- Alumina coating is highly preventing the concentration of the corrosion salts due to absence of

concentration centers such as interconnected cracks, porosity and voids.

6- The plasma sprayed coating with YSZ shows a lower resistance to salts attack compared with the sample of YSZ/Al2O3 composite.

**References**

1. Pawlowski and Lech, The Science and Engineering of Thermal Spray Coatings:, John Wiley & Sons, 2008.

2. M. Wank, H. Steffens and M. Brune, "New thermal barrier coating system for high temperature applications," in 15th International Thermal Spray Conference, Nice, France, May 1998.

3. R. W. Smith and R. Knight, "Thermal Spraying I: Powder Consolidation-From Coating to Forming," The Journal of The Minerals, Metals & Materials Society, vol. 47, no. 8, pp. 31-39, 1995

4. H. Herman and S. Sampath, "Thermal Spray: Current Status and Future Trends," Jornal of Materials Research Society Bulletin, vol. 25, no. 7, pp. 17-25, 2011.

5. D.Wortman and B. Nagaraj, "Thermal Barrier Coatings for Gas Turbine Use," Materials Science and Engineerin, vol. A I21, pp. 433-440, 1989.

**6.** C. Zhang, H.Peng and S. Gong, "Influence of thermal shock on insulation effect of nano-multilayer thermal barrier coatings," Surface & Coatings Technology, vol. 201, p. 6340–6344, 2007.

**7.** X. Liu, C. Wang and Y. Wang, "Improving oxidation resistance and thermal insulation of thermal barrier coatings by intense pulsed electron beam irradiation," Applied Surface Science Journal,vol. 263, p. 810–815, 2012.

**8.** A. Keyvani, M. Sarem and M. Sohi, "An investigation on oxidation, hot corrosion and mechanical properties of plasma-sprayed conventional and nanostructured YSZ coatings," Surface & Coatings Technology , vol. 206, p. 208–216, 2011.

**9.** Z. Liu, J. Ouyang, Y. Zhou and S. Li, "High-temperature hot corrosion behavior of gadolinium zirconate by vanadium pentoxide and sodium sulfate in air," Journal

of the European Ceramic Society , vol. 30, p. 2707–2713, 2010.

10. H. Jamali, R. Mozafarinia, R. Razavi and R. Pidani, “Comparison of hot corrosion behaviors of plasma-sprayed nanostructured and conventional YSZ thermal barrier coatings exposure to molten vanadium pentoxide and sodium sulfate,” Journal of the European Ceramic Society , vol. 34, p. 485–492, 2014

11. E. Adolfsson, P.Henning and L. Hermansson, “Phase Analysis and Thermal Stability of Hot Isostatically Pressed Zirconia–Hydroxyapatite Composites,” Journal of American Ceramic Society, vol. 83, no. 11, p. 2798–802, 2000.

12. M. Daroonparvar, M. Yajid and N. Yusof, “Investigation of three steps of hot corrosion process in Y2O3 stabilized ZrO2 coatings including nano zones,” Journal of Rare Earths, vol. 32, no. 10, pp. 989-1002, 2014.

13. H. Habibi and S. Guo, “Evolution of Hot Corrosion Behavior of YSZ-Ta2O5 Composites with Different YSZ/Ta2O5 Ratios,” Journal of

Applied Cerammic Technology, vol. 12, no. 3, pp. 542-550, 2015.

14. M. Estarkia and o. M. Nejatib, “Evaluation of hot corrosion behavior of plasma sprayed scandia and yttria co-stabilized nanostructured thermal barrier coatings in the presence ofmolten sulfate and vanadate salt,” Journal of the European Ceramic Society,p. Article in Press, 2017.

15. M. Habibia, S.Yang and S.Guoa, “Phase stability and hot corrosion behavior of ZrO2–Ta2O5 compound in Na2SO4–V2O5mixtures atelevatedtemperatures,” Ceramics International Journal, vol. 40, p. 4077–4083, 2014.

16. S. Das, S. Datta, D. Basu and G. Das, “Glass–ceramics as oxidation resistant bond coat in thermal barrier coating system,” Ceramics International Journal , vol. 35, p. 1403–1406, 2009.

17. W.Gong, C. Sha and D. Sun, “Microstructures and thermal insulation capability of plasma-sprayed nanostructured ceria stabilized zirconia coatings,” Surface & Coatings

Technology Journal , vol. 201, p. 3109–3115, 2006.

18. R. Pidanin, R. Razavi, R. Mozafarinia and H. Jamali, “Evaluation of hot corrosion behavior of plasma sprayed ceria and yttria stabilized zirconia thermal barrier coatings in the presence of Na2SO4+V2O5molten salt,” Ceramics International Journal , vol. 38, p. 6613–6620, 2012.

19. N. Padture, M. Gell and H. jordan, “Thermal barrier coatings for gas turbine engine applications,” Material Science Journal, vol. 296, p. 280–284, 2002.

20. L. Pejryd and J. Wigren, “Thermal barrier coatings- why, how, where and where to,” in 15th International Thermal Spray Conference, Nice, France, 1998.

21. G. Keijzers, “Thermal Spray Coatings and High Performance Engine Valves,” Journal of International Thermal Spray & Surface Engineering, vol. 5, no. 3, pp. 42-43, August 2010.

22. R. Ghasemi, R. Razavi, R. Mozafarinia, H. Jamali and R. Pidani, “The influence of laser treatment on hot corrosion behavior of plasma-sprayed nanostructured yttria stabilized zirconia thermal barrier coatings,” Journal of the European Ceramic Society, vol. 34, p. 2013–2021, 2014.

23. R. Ghasemi, R. Razavi, R. Mozafarinia and H. Jamalia, “Comparison of microstructure and mechanical properties of plasma-sprayed nanostructured and conventional yttria stabilized zirconia thermal barrier coatings,” Ceramics International Journan, vol. Accepted Manuscript, pp. 1-26, 2013.

24. Z. Fan, K. Wang, X. Dong, R. Wang, W. Duan and X. Mei, “Effect of Ultrasonic Vibration on Microstructure and Corrosion Resistance of Laser Re-Melted Thermal Barrier Coatings,” in International Conference on Surface Modification Technologies, Milan, Italy, 2016.

25. K. Prasad, S. Mukherjee, K. Antony and M. Manikandan, “Investigation on Hot Corrosion Behavior of Plasma Spray Coated Nickel Based Superalloy in Aggressive

Environments at 900°C," International Journal of ChemTech Research, vol. 6, no. 1, pp. 416-431, 2014.

26. M. Nejati, M.Rahimipour and I. Mobasherpour, "Evaluation of hot corrosion behavior of CSZ,CSZ/microAl2O3 and CSZ/nanoAl2O3 plasma sprayed thermal barrier coatings," Ceramics International Journal, vol. 40, p. 4579–4590, 2014.

27. "Hot Corrosion Mechanism of Composite Alumina/Yttria-Stabilized Zirconia Coating in Molten Sulfate–Vanadate Salt," Journal of the American Ceramic Society,vol. 88, no. 3, p. 675–682, 2005.

28. H. Chen, Z. L. i. u and Y. Chuang, "Degradation of plasma-sprayed alumina and zirconia coatings on stainless steel during thermal cycling and hot corrosion," Thin Solid Films journal 223, vol. 223, pp. 56-64, 1992.

29. M. H. Habibi, Hot Corrosion Behaviour of New Candidates for Thermal Barrier Coatings Application in Turbine Simulated Environments,Louisiana State University: PhD Dissertation, 2014.

30. P.Mohan, B. Yuan, T. Patterson and V. Desai, "Degradation of Yttria-Stabilized Zirconia Thermal Barrier Coatings by Vanadium Pentoxide,Phosphorous, Pentoxide, and Sodium Sulfate," Journal of the American Ceramic Society,vol. 90, no. 11, p. 3601–3607, 2007.

31. M. Habibi and S. G. Li Wang, "Evolution of hot corrosion resistance of YSZ, Gd2Zr2O7, and Gd2Zr2O7 + YSZ composite thermal barrier coatings in Na2SO4 + V2O5 at 1050 ◦C," Journal of the European Ceramic Society, vol. 32, pp. 1635-1642, 2012.

32. S. Saladi, J. Menghani and S. Prakash, "Hot Corrosion Behaviour of Detonation-Gun Sprayed Cr3C2–NiCr Coating on Inconel-718 in Molten Salt Environment at 900 °C," Transactions of the Indian Institute of Metals, vol. 76, no. 5, p. 623–627 , 2014.

33. M. Habibi, L. Wang, J. Liang and S. Guo, "An investigation on hot corrosion behavior of YSZ-Ta2O5 in Na2SO4 + V2O5
salt at 1100 oC," Journal of Corrosion Science , vol. 75, p. 409–414, 2013.

34. L. Klinkova and E. Ukshe, "'Solution of Corundum in Fused Vanadates," Russian Journal ofof Inorganic Chemistry,vol. 20, no. 2, p. 799–803, 1975.